W&M ScholarWorks

Arts & Sciences Articles

Arts and Sciences

2012

Polarization Components in pi(0) Photoproduction at Photon Energies up to 5.6 GeV

W. Luo

B. Hu

X. Zhang

M. Meziane
William & Mary

L. Pentchev
William & Mary

See next page for additional authors

Recommended Citation

Luo, W.; Hu, B.; Zhang, X.; Meziane, M.; Pentchev, L.; and Perdrisat, C. F., Polarization Components in pi(0) Photoproduction at Photon Energies up to 5.6 GeV (2012). *Physical Review Letters*, 108(22). 10.1103/PhysRevLett.108.222004

Authors

W. Luo, B. Hu, X. Zhang, M. Meziane, L. Pentchev, and C. F. Perdrisat

P H Y S I C A L   R E V I E W   L E T T E R S

Polarization Components in π^0 Photoproduction at Photon Energies up to 5.6 GeV

W. Luo,[1] E. J. Brash,[2,3] R. Gilman,[3,4] M. K. Jones,[3] M. Meziane,[5] L. Pentchev,[5] C. F. Perdrisat,[5] A. J. R. Puckett,[6,7] V. Punjabi,[8] F. R. Wesselmann,[8] A. Ahmidouch,[9] I. Albayrak,[10] K. A. Aniol,[11] J. Arrington,[12] A. Asaturyan,[13] O. Ates,[10] H. Baghdasaryan,[14] F. Benmokhtar,[15] W. Bertozzi,[6] L. Bimbot,[16] P. Bosted,[3] W. Boeglin,[17] C. Butuceanu,[18] P. Carter,[2] S. Chernenko,[19] M. E. Christy,[10] M. Commisso,[14] J. C. Cornejo,[11] S. Covrig,[3] S. Danagoulian,[9] A. Daniel,[20] A. Davidenko,[21] D. Day,[14] S. Dhamija,[17] D. Dutta,[22] R. Ent,[3] S. Frullani,[23] H. Fenker,[3] E. Frlez,[14] F. Garibaldi,[23] D. Gaskell,[3] S. Gilad,[6] Y. Goncharenko,[21] K. Hafidi,[12] D. Hamilton,[24] D. W. Higinbotham,[3] W. Hinton,[8] T. Horn,[3] B. Hu,[1,*] J. Huang,[6] G. M. Huber,[18] E. Jensen,[2] H. Kang,[25] C. Keppel,[10] M. Khandaker,[8] P. King,[20] D. Kirillov,[19] M. Kohl,[10] V. Kravtsov,[21] G. Kumbartzki,[4] Y. Li,[10] V. Mamyan,[14] D. J. Margaziotis,[11] P. Markowitz,[17] A. Marsh,[2] Y. Matulenko,[21,†] J. Maxwell,[14] G. Mbianda,[26] D. Meekins,[3] Y. Melnik,[21] J. Miller,[27] A. Mkrtchyan,[13] H. Mkrtchyan,[13] B. Moffit,[6] O. Moreno,[11] J. Mulholland,[14] A. Narayan,[22] Nuruzzaman,[22] S. Nedev,[28] E. Piasetzky,[29] W. Pierce,[2] N. M. Piskunov,[19] Y. Prok,[2] R. D. Ransome,[4] D. S. Razin,[19] P. E. Reimer,[12] J. Reinhold,[17] O. Rondon,[14] M. Shabestari,[14] A. Shahinyan,[13] K. Shestermanov,[21,†] S. Širca,[30] I. Sitnik,[19] L. Smykov,[19,†] G. Smith,[3] L. Solovyev,[21] P. Solvignon,[12] I. I. Strakovsky,[31] R. Subedi,[14] R. Suleiman,[3] E. Tomasi-Gustafsson,[32,16] A. Vasiliev,[21] M. Veilleux,[2] S. Wood,[3] Z. Ye,[10] Y. Zanevsky,[19] X. Zhang,[1] Y. Zhang,[1] X. Zheng,[14] and L. Zhu[10]

(GEp-III and GEp2γ Collaborations)

[1]*Lanzhou University, Lanzhou 730000, Gansu, People's Republic of China*
[2]*Christopher Newport University, Newport News, Virginia 23606, USA*
[3]*Thomas Jefferson National Accelerator Facility, Newport News, Virginia 23606, USA*
[4]*Rutgers, The State University of New Jersey, Piscataway, New Jersey 08855, USA*
[5]*The College of William and Mary, Williamsburg, Virginia 23187, USA*
[6]*Massachusetts Institute of Technology, Cambridge, Massachusetts 02139, USA*
[7]*Los Alamos National Laboratory, Los Alamos, New Mexico 87545, USA*
[8]*Norfolk State University, Norfolk, Virginia 23504, USA*
[9]*North Carolina A&T State University, Greensboro, North Carolina 27411, USA*
[10]*Hampton University, Hampton, Virginia 23668, USA*
[11]*California State University, Los Angeles, Los Angeles, California 90032, USA*
[12]*Argonne National Laboratory, Argonne, Illinois 60439, USA*
[13]*Yerevan Physics Institute, Yerevan 375036, Armenia*
[14]*University of Virginia, Charlottesville, Virginia 22904, USA*
[15]*Carnegie Mellon University, Pittsburgh, Pennsylvania 15213, USA*
[16]*Institut de Physique Nucléaire, CNRS, IN2P3 and Université Paris Sud, Orsay Cedex, France*
[17]*Florida International University, Miami, Florida 33199, USA*
[18]*University of Regina, Regina, Saskatchewan S4S OA2, Canada*
[19]*JINR-LHE, Dubna, Moscow Region, Russia 141980*
[20]*Ohio University, Athens, Ohio 45701, USA*
[21]*IHEP, Protvino, Moscow Region, Russia 142284*
[22]*Mississippi State University, Starkeville, Mississippi 39762, USA*
[23]*INFN, Sezione Sanità and Istituto Superiore di Sanità, 00161 Rome, Italy*
[24]*University of Glasgow, Glasgow G12 8QQ, Scotland, United Kingdom*
[25]*Seoul National University, Seoul 151-742, South Korea*
[26]*University of Witwatersrand, Johannesburg, South Africa*
[27]*University of Maryland, College Park, Maryland 20742, USA*
[28]*University of Chemical Technology and Metallurgy, Sofia, Bulgaria*
[29]*University of Tel Aviv, Tel Aviv, Israel*
[30]*Jozef Stefan Institute, 3000 SI-1001 Ljubljana, Slovenia*
[31]*The George Washington University, Washington, D.C. 20052, USA*
[32]*CEA Saclay, F-91191 Gif-sur-Yvette, France*

We present new data for the polarization observables of the final state proton in the $^1H(\vec{\gamma}, \vec{p})\pi^0$ reaction. These data can be used to test predictions based on hadron helicity conservation and perturbative QCD. These data have both small statistical and systematic uncertainties and were obtained with beam energies between 1.8 and 5.6 GeV and for π^0 scattering angles larger than 75° in the center-of-mass

frame. The data extend the polarization measurements database for neutral pion photoproduction up to $E_\gamma = 5.6$ GeV. The results show a nonzero induced polarization above the resonance region. The polarization transfer components vary rapidly with the photon energy and π^0 scattering angle in the center-of-mass frame. This indicates that hadron helicity conservation does not hold and that the perturbative QCD limit is still not reached in the energy regime of this experiment.

One of the major goals of nuclear physics is to understand the mechanism of exclusive reactions, like meson photoproduction. Nuclear reactions are described by meson-exchange models at low energy, and perturbative QCD (pQCD) is expected to apply at very high energy. The reaction dynamics of the transition remain unclear in the intermediate energy regime. The constituent counting rule (CCR) [1] and hadron helicity conservation (HHC) [2] can be considered as indications of the applicability of pQCD. A scaling behavior for a variety of differential cross sections has been observed for many exclusive reactions [3–9] as predicted by the CCR. But the onset of scaling sometimes starts at the surprisingly low energy of 1 GeV, where pQCD should not work. The limited experimental data do not support the validity of HHC in the few GeV regime. Another unsolved problem is that, although quark models explain well the baryon excitation states below 2 GeV, these theories also predict a large density of resonance states at higher energy which have not been observed yet [10]. Measurements of both cross section and polarization observables help the understanding of the dynamics of exclusive reactions.

Prominent structures in the cross section data indicate that π^0 photoproduction is dominated by the excitation of baryon resonances at low photon energies $E_\gamma < 1.8$ GeV. Above the known resonance region, the cross section becomes structureless and approximately follows CCR. Two observables, the induced recoil proton polarization P and the linearly polarized photon asymmetry Σ, which are well characterized below 1.5 GeV, provide further evidence of the dominance of resonance excitation in the $E_\gamma < 1.8$ GeV region. A Jefferson Lab Hall A experiment [11] has obtained data for the three recoil proton polarization components and confirmed the importance of polarization observables as a powerful tool in the search for resonance states. The contribution of these polarization results in constraining multipole analyses was investigated in Ref. [12], and the conclusion was that more data were needed to constrain the multipoles above 1 GeV. The structureless cross section data do not rule out the possibility of overlapping high-mass resonance states with large width. High precision measurement of polarization observables may give hints to the existence of missing baryon resonance states.

As a consequence of pQCD and with the assumption that orbital angular momentum can be neglected, HHC predicts that the polarization components of the proton above the baryon resonance region should have a smooth dependence on E_γ and approach limits established by HHC in the absence of baryon resonances in the $^1H(\vec{\gamma}, \vec{p})\pi^0$ reaction. The results from Ref. [11] have demonstrated that HHC is not valid up to 3 GeV. Huang *et al.* [13] calculated the polarization observables in pion photoproduction by assuming the handbag mechanism. However, the theoretical calculation could not be compared to the data, because the photon energy of Ref. [11] is not high enough for the handbag mechanism to be applicable. In the past several years, it has become increasingly apparent that orbital angular momentum cannot generally be neglected in high energy reactions [14,15]. This has led to an extension of the CCR to include orbital angular momentum effects, but to date there are no predictions for the effects of orbital angular momentum on polarization observables. In the absence of resonances, any energy dependence is likely small, but strong angle variations might persist. The present work measured the three polarization observables in high precision up to 5.6 GeV.

Two experiments were carried out by the GEp-III and GEp-2γ Collaborations in Hall C at Jefferson Lab. GEp-III measured the elastic proton form factor ratio to high four-momentum transfer, Q^2, by using the recoil polarization method in the ep elastic reaction [16]. GEp-2γ measured the kinematic dependence of the ratio at fixed Q^2 [17]. Because of its relatively larger cross section at high Q^2 and kinematical similarity in phase space to the ep elastic reaction, neutral pion production was the major contribution to the background of these experiments. The other reactions are suppressed by the ep elastic kinematic settings. These pions come from real photoproduction as well as electroproduction. The angular and energy selectivity of these experiments restricted the contribution of electroproduction to very low values of Q^2, i.e., quasireal photons, resulting in final states indistinguishable from photoproduction induced by real bremsstrahlung photons. Therefore, the polarization observables of the protons in these two reactions are similar as proven by a previous experiment [11]. In this Letter, these two reaction channels are not distinguished and are collectively called neutral pion photoproduction.

A high luminosity longitudinally polarized electron beam (79%–86% polarization) was scattered from a 20 cm liquid hydrogen target. In the six kinematic settings of the experiments, the incident electron energy was 1.87, 2.84, 3.63, 4.05, and 5.71 GeV (two settings with

$E_e = 5.71$ GeV). The beam helicity was flipped at 30 Hz. The beam polarization was monitored by the Hall C Møller polarimeter [18] with an accuracy of 1.0%. Near the end point, the circular polarization of the bremsstrahlung photons is nearly equal to the longitudinal polarization of the incident electron, while the linear polarization component vanishes [19].

The scattered protons were detected in the Hall C High Momentum Spectrometer (HMS) [20]. The proton trajectories were measured by drift chambers in the HMS focal plane. The polarization of the proton was measured by the focal plane polarimeter in the HMS detector hut downstream from the HMS drift chambers. The focal plane polarimeter, consisting of two 55 cm CH_2 analyzer blocks, each followed by a pair of drift chambers, measured the asymmetry of the charged particles in $\vec{p} + CH_2 \rightarrow$ charged particle $+ X$ to extract the proton polarization.

An electromagnetic calorimeter (BigCal), with a front area of 1.2×2.2 m^2 and consisting of 1744 lead-glass blocks, was placed at the six positions matching the acceptance of the HMS for the elastic ep reaction. BigCal provides no discrimination between electrons and photons and gives the impact position with similar resolution for both. The BigCal energy resolution changed from $10\%/\sqrt{E}$ to $23\%/\sqrt{E}$ during the experiment due to radiation damage. By contrast, the coordinate resolution of about 8 mm is not measurably affected by radiation damage. The primary trigger of the experiment was a coincidence between signals from the BigCal and from the HMS within a ± 50 ns timing window.

In π^0 photoproduction, the meson decays into two photons directly following its production. The minimum opening angle between these two decay photons corresponds to the two photons sharing the energy of the π^0 equally in the lab frame. As the opening angle increases, one photon will take more energy from the π^0, and its track will be closer to the incident π^0 track direction. Either of the π^0 decay photons with energy greater than the BigCal hardware energy threshold (set typically at about half the ep elastic scattered electron energy) hitting the BigCal will produce a BigCal trigger. If the event was in coincidence with a proton in the HMS, it was recorded. In two kinematic settings where the electron beam energy was 5.71 GeV, the BigCal coincidence acceptance with the HMS was large enough to detect both photons. These data with lower statistics were also analyzed, and the results were found to be consistent with the "one photon detected" results. In this Letter, only the one photon detected results will be shown.

To identify π^0 events when one photon was detected in the BigCal, the π^0 decay photon energy predicted from the proton angle, momentum, and the π^0 decay photon angle was compared with the energy measured in the BigCal. A good linear correlation was seen between the measured and predicted energies. We applied a 3σ cut on the ratio of the measured and predicted photon energy to identify the π^0 events. The major background events in the π^0 photoproduction channel come from the ep elastic radiative tail and from random coincidence events. To reduce random background, a 3σ cut around the BigCal and HMS coincidence time peak was applied. The ep elastic radiation tail contamination was estimated by comparing the data to Monte Carlo simulation. Background events came from heavier meson photoproduction, and multiple π^0 photoproductions were also estimated by the simulation. Only the data near the bremsstrahlung end point with less than 1.0% contamination from these two types of reactions were kept in the analysis.

Figure 1 shows the distribution of the predicted π^0 decay photon energy E'_{calo}. The left vertical dashed line indicates the hardware energy threshold of BigCal, and the right vertical dashed line indicates the E'_{calo} upper limit selected to optimize the signal to background ratio and statistics. Events between the two vertical dashed lines were selected and used in the analysis. At an incident photon energy of 3.951 GeV, the elastic background contamination ratio in the selected range of E'_{calo} is 1.2%, and the random background contamination is 1.5% after all cuts were applied. The polarization components of both kinds of background were studied separately, and corrections were applied to the final results.

Elastic events were used to calibrate the focal plane polarimeter analyzing power and determine the instrumental asymmetry at each kinematic setting. With the knowledge of the beam polarization and of the spin precession in
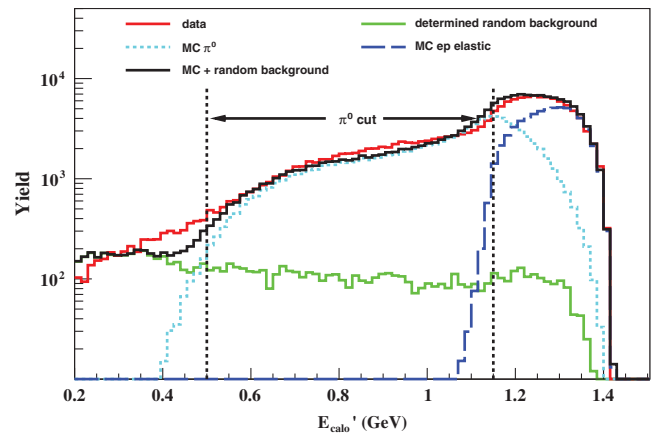

FIG. 1 (color). The π^0 event selection at an incident photon energy $E_\gamma = 3.951$ GeV. The distributions of the predicted energy deposition in the BigCal are plotted for the data (red solid line), the random background (green solid line) determined from time of flight spectra, the Monte Carlo simulation of π^0 events (light blue dotted line), and the MC simulation of ep elastic events (blue dashed line). The black solid line is the sum of the MC simulation of π^0's, ep elastic events, and the measured random background. The simulated curves have been scaled to match the data. The two vertical lines are described in the text.

the HMS [21], polarization transfer in the ep elastic reaction allows the determination of both the CH_2 analyzing power and the ratio of the proton electromagnetic form factors. To take into account the proton momentum difference between elastic events and π^0 events, the analyzing power of π^0 events was obtained by correcting the ep elastic results according to the analyzing power momentum dependence [22]. As the induced polarization in ep elastic scattering is zero in the one photon exchange mechanism, the instrumental asymmetry could be extracted by Fourier analysis of the helicity sum spectrum of ep elastic events. The same cut on hit position of the protons in the focal plane of ep elastic events was applied to the π^0 events to make sure the calibrated analyzing power and the instrumental asymmetry are valid. This cut also further suppressed the heavier meson (e.g., η) production contribution to the data by requiring higher proton momentum in the HMS. After all these calibrations were done, the induced and transferred polarization components of the proton in π^0 photoproduction at the target were extracted by the maximum likelihood method described in Ref. [16].

The high statistics of π^0 events allows us to divide the data into several incident photon energy bins. The bin size was selected to be greater than the reconstructed incident photon energy resolution and to keep enough events to calculate the polarization components in each bin. Systematic uncertainties were estimated by analyzing the sensitivity of the polarization components to background corrections, the beam polarization, the instrumental asymmetry, the analyzing power calibration, and the tracking reconstruction systematics for each bin. For the polarization transfer components, the uncertainties from the ep elastic background estimation are dominant, because the polarization is very different in ep elastic events. The systematic uncertainties of the induced polarization

component are dominated by the instrumental asymmetry correction. Overall, the systematic uncertainties are less than ±0.026 for the polarization transfer components and do not exceed ±0.034 for the induced polarization component.

The results are listed in Table I. No induced polarization data for the last kinematics in the table are available, because the spin precession inside the HMS at this setting leads to very large systematic uncertainties. The lab coordinate system is defined by $\hat{z} = \hat{k}_{\mathrm{proton}}/|\hat{k}_{\mathrm{proton}}|$, $\hat{y} = \hat{k}_{\mathrm{proton}} \times \hat{k}_\gamma/|\hat{k}_{\mathrm{proton}} \times \hat{k}_\gamma|$, and $\hat{x} = \hat{y} \times \hat{z}$, where $\hat{k}_{\mathrm{proton}}$ $(\hat{k}_\gamma)$ is the recoil proton (incident photon) momentum. C_z^{lab}, P, and C_x^{lab} are the longitudinal, the induced (along $\hat{y}$), and the transverse polarization components in the lab system, respectively.

Several theoretical models predict the polarization observables in the $^1H(\vec{\gamma}, \vec{p})\pi^0$ reaction; they are partial-wave analyses Scattering Analysis Interactive Database (SAID) [23] and Mainz unitary isobar model [24] ($E_\gamma \leq$ 1.65 GeV), a quark model subprocess calculation by Afanasev, Carlson, and Wahlquist [25], and a pQCD prediction from Farrar, Huleihel, and Zhang [26].

In SAID, both an energy-dependent and a set of energy-independent partial-wave analyses of single-pion photoproduction data were performed. The latest solution (SP09) [27] extends from threshold to 2.7 GeV of incident photon energy in the laboratory.

Assuming helicity conservation, the induced polarization P and the transverse polarization transfer $C_x^{\mathrm{c.m.}}$ in pion photoproduction are zero. From pQCD scaling arguments, the longitudinal polarization transfer $C_z^{\mathrm{c.m.}}$ is constant at fixed $\theta_\pi^{\mathrm{c.m.}}$, but HHC alone does not determine the value of this constant.

Farrar, Huleihel, and Zhang predicted the helicity amplitudes for pion photoproduction by explicitly calculating all lowest-order Feynman diagrams [26]. Several nucleon

TABLE I. The proton polarization components for the process $^1H(\vec{\gamma}, \vec{p})\pi^0$. The E_γ is the incident photon energy calculated by the proton angle and momentum, $\theta_{\pi^0}^{\mathrm{c.m.}}$ is the angle of π^0 in c.m. frame for each bin of E_γ, and χ is the proton spin precession angle inside the HMS.

$\bar{E}_\gamma$ (GeV)	$\bar{\theta}_{\pi^0}^{\mathrm{c.m.}}$ (deg)	$\bar{\chi}$ (deg)	$C_x^{\mathrm{lab}} \pm$ stat $\pm$ syst	$C_z^{\mathrm{lab}} \pm$ stat $\pm$ syst	$P \pm$ stat $\pm$ syst
1.845 ± 0.038	143.3 ± 2.5	108.9	$0.331 \pm 0.003 \pm 0.006$	$0.073 \pm 0.006 \pm 0.005$	$-0.503 \pm 0.014 \pm 0.012$
2.704 ± 0.050	97.1 ± 2.3	108.9	$0.508 \pm 0.007 \pm 0.005$	$0.255 \pm 0.013 \pm 0.004$	$0.138 \pm 0.030 \pm 0.009$
2.776 ± 0.025	96.1 ± 2.3		$0.465 \pm 0.009 \pm 0.005$	$0.263 \pm 0.017 \pm 0.003$	$0.023 \pm 0.036 \pm 0.009$
3.304 ± 0.050	82.5 ± 2.3	108.9	$0.082 \pm 0.014 \pm 0.009$	$0.358 \pm 0.024 \pm 0.009$	$0.215 \pm 0.053 \pm 0.014$
3.402 ± 0.050	81.6 ± 2.5		$0.074 \pm 0.008 \pm 0.009$	$0.362 \pm 0.014 \pm 0.009$	$0.210 \pm 0.030 \pm 0.012$
3.498 ± 0.050	79.7 ± 2.3		$0.080 \pm 0.009 \pm 0.008$	$0.343 \pm 0.016 \pm 0.008$	$0.151 \pm 0.034 \pm 0.010$
3.569 ± 0.030	79.4 ± 2.5		$0.094 \pm 0.018 \pm 0.008$	$0.293 \pm 0.031 \pm 0.010$	$0.237 \pm 0.066 \pm 0.012$
3.858 ± 0.050	124.7 ± 4.2	176.0	$0.061 \pm 0.024 \pm 0.007$	$0.742 \pm 0.077 \pm 0.020$	$-0.176 \pm 0.020 \pm 0.011$
3.951 ± 0.050	123.3 ± 4.6		$0.064 \pm 0.018 \pm 0.003$	$0.699 \pm 0.057 \pm 0.018$	$-0.174 \pm 0.015 \pm 0.009$
5.550 ± 0.050	112.6 ± 4.0	219.5	$0.098 \pm 0.041 \pm 0.007$	$-0.078 \pm 0.080 \pm 0.009$	$0.387 \pm 0.053 \pm 0.034$
5.631 ± 0.030	112.2 ± 5.3		$0.025 \pm 0.054 \pm 0.002$	$-0.162 \pm 0.104 \pm 0.009$	$0.347 \pm 0.070 \pm 0.033$
5.552 ± 0.050	138.1 ± 4.0	261.6	$0.198 \pm 0.015 \pm 0.021$	$0.732 \pm 0.016 \pm 0.026$	
5.643 ± 0.040	137.3 ± 5.3		$0.189 \pm 0.016 \pm 0.009$	$0.772 \pm 0.017 \pm 0.019$	

and pion wave functions were used in the calculation. The predicted cross sections are highly sensitive to the choices of wave functions, and they do not agree with the data in general. The calculated curves shown in Fig. 2 used asymptotic distribution amplitudes for both the proton and the pion.

Afanasev, Carlson, and Wahlquist [25] used a pQCD approach to calculate the longitudinal polarization $C_z^{c.m.}$ of meson photoproduction in the limit $x_{Bjorken} \rightarrow 1$. This model assumes helicity conservation and that the pQCD approach is justified for high meson transverse momentum.

Figure 2 presents the comparison of the new Hall C results with data from previous experiment and the available models. Not all the data of Ref. [11] are shown in the figure. The theoretical predictions are calculated for the given π^0 center-of-mass (c.m.) angles shown in the panels and have been converted from the c.m. frame to the lab frame. In the lower incident photon energy regime ($E_\gamma <$ 2.7 GeV), these new data agree with the world data except for the induced polarization in Fig. 2(j). A strong $\theta_\pi^{c.m.}$ dependence for P at $E_\gamma = 2.5$ GeV was found in the previous measurement [11]. The polarization dependence on $\theta_\pi^{c.m.}$ at $E_\gamma = 2.7$ GeV is studied, and the results show a compatible oscillation comparing to Ref. [11] for P and C_x^{lab}. This discrepancy very likely comes from the difference in $\theta_\pi^{c.m.}$ between the new data and the previous measurement. While the SAID model gives good overall predictions for energies lower than 3 GeV, it disagrees with the data in Figs. 2(a), 2(h), and 2(j); this can be understood, since above 1 GeV the multipoles are still underconstrained in the model. For the larger incident

photon energies ($E_\gamma > 3.0$ GeV), the new data are the first measurements at the given $\theta_\pi^{c.m.}$. The results still show strong energy dependence in C_z^{lab} and P at 120° and a strong angle dependence in C_z^{lab} at $E_\gamma \approx 5.6$ GeV. Such behavior was not predicted by the models based on HHC. It appears, based on our few examples, that the strong kinematic dependences in the SAID fit at low energies continue up to 5.6 GeV.

In conclusion, the precise new polarization data for π^0 photoproduction from the proton presented here extend the world data set to $E_\gamma = 5.6$ GeV. In the lower energy region, the new data are in good agreement with previous measurements and the SAID predictions. The new data for $E_\gamma < 2.7$ GeV together with data from Mainz Microtron C [28] will give further constraint on the multipole fit above 1 GeV. At higher energy, the new data show no evidence of HHC up to $E_\gamma = 5.6$ GeV. Furthermore, the polarization transfer components vary drastically as a function of $\theta_\pi^{c.m.}$ at $E_\gamma \approx 5.6$ GeV, and this is not predicted by any theoretical model. The high energy data may allow interpretation in terms of the quark handbag mechanism, providing access to polarization-dependent generalized parton distributions, as discussed in Refs. [13,29]. More theoretical predictions would be highly desirable, and the interpretation of the data would help achieve a complete understanding of the mechanism of this reaction.

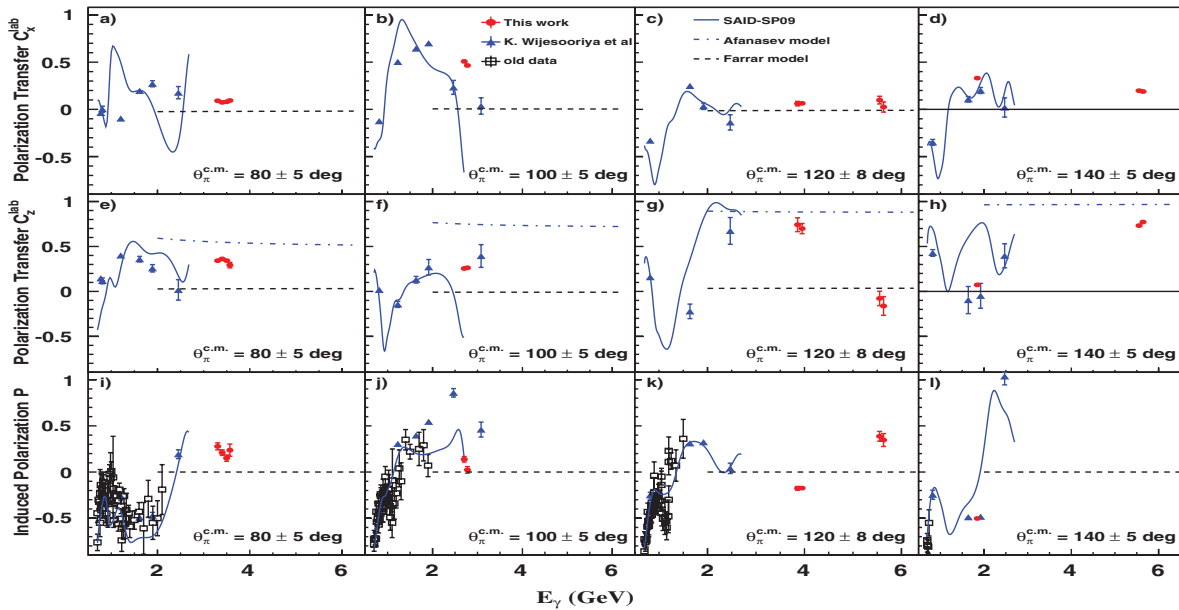FIG. 2 (color). Top to bottom: Polarization transfer C_x^{lab}, C_z^{lab}, and induced polarization P in the lab frame. Left to right: Different angles of π^0 in the c.m. frame. The "old data" could be found in the SAID database [23]. The three curves labeled Afanasev model [25], Farrar model [26], and SAID SP09 [27] are described in the text. Only the statistical uncertainties are shown.

*Corresponding author.
hubt@lzu.edu.cn
†Deceased.

[1] S. J. Brodsky and G. R. Farrar, Phys. Rev. Lett. **31**, 1153 (1973).

[2] S. J. Brodsky and G. P. Lepage, Phys. Rev. D **24**, 2848 (1981).

[3] R. L. Anderson, D. B. Gustavson, D. M. Ritson, G. A. Weitsch, H. J. Halpern, R. Prepost, D. H. Tompkins, and D. E. Wiser, Phys. Rev. D **14**, 679 (1976).

[4] C. Bochna et al., Phys. Rev. Lett. **81**, 4576 (1998).

[5] J. E. Belz et al., Phys. Rev. Lett. **74**, 646 (1995).

[6] S. J. Freedman et al., Phys. Rev. C **48**, 1864 (1993).

[7] E. C. Schulte et al., Phys. Rev. Lett. **87**, 102302 (2001).

[8] L. Y. Zhu et al. (Jefferson Lab Hall A Collaboration), Phys. Rev. Lett. **91**, 022003 (2003).

[9] W. Chen et al. (CLAS Collaboration), Phys. Rev. Lett. **103**, 012301 (2009).

[10] E. Klempt and J.-M. Richard, Rev. Mod. Phys. **82**, 1095 (2010).

[11] K. Wijesooriya et al., Phys. Rev. C **66**, 034614 (2002).

[12] R. A. Arndt, I. I. Strakovsky, and R. L. Workman, Phys. Rev. C **67**, 048201 (2003).

[13] H. W. Huang, R. Jakob, P. Kroll, and K. Passek-Kumericki, Eur. Phys. J. C **33**, 91 (2004).

[14] X. Ji, J.-P. Ma, and F. Yuan, Phys. Rev. Lett. **90**, 241601 (2003).

[15] D. Dutta and H. Gao, Phys. Rev. C **71**, 032201 (2005).

[16] A. J. R. Puckett et al., Phys. Rev. Lett. **104**, 242301 (2010).

[17] M. Meziane et al. (GEp2γ Collaboration), Phys. Rev. Lett. **106**, 132501 (2011).

[18] M. Hauger et al., Nucl. Instrum. Methods Phys. Res., Sect. A **462**, 382 (2001).

[19] H. Olsen and L. C. Maximon, Phys. Rev. **114**, 887 (1959).

[20] H. Blok et al. (Jefferson Lab Fπ Collaboration), Phys. Rev. C **78**, 045202 (2008).

[21] K. Makino and M. Berz, Nucl. Instrum. Methods Phys. Res., Sect. A **427**, 338 (1999).

[22] L. S. Azghirey et al., Nucl. Instrum. Methods Phys. Res., Sect. A **538**, 431 (2005).

[23] R. A. Arndt, W. J. Briscoe, I. I. Strakovsky, and R. L. Workman, Phys. Rev. C **66**, 055213 (2002).

[24] D. Drechsel, S. Kamalov, and L. Tiator, Eur. Phys. J. A **34**, 69 (2007).

[25] A. Afanasev, C. E. Carlson, and C. Wahlquist, Phys. Lett. B **398**, 393 (1997).

[26] G. R. Farrar, K. Huleihel, and H. Zhang, Nucl. Phys. **B349**, 655 (1991).

[27] M. Dugger et al. (CLAS Collaboration), Phys. Rev. C **79**, 065206 (2009).

[28] M. Sikora, Ph.D. thesis, Edinburgh University, 2011.

[29] A. V. Afanasev, arXiv:hep-ph/9808291.